

## Influence of the boundary resistivity on the proximity effect

C. Ciuhu and A. Lodder

*Faculty of Sciences / Natuurkunde en Sterrenkunde, Vrije Universiteit, De Boelelaan 1081, 1081 HV Amsterdam, The Netherlands*

(Received 22 June 2001; published 26 November 2001)

We apply the theory of Takahashi and Tachiki in order to explain theoretically the dependence of the upper critical magnetic field of a S/N multilayer on the temperature. This problem has been already investigated in the literature, but with a use of an unphysical scaling parameter for the coherence length. We show explicitly that, in order to describe the data, such an unphysical parameter is unnecessary if one takes into account the boundary resistivity of the S/N interface. We obtain a very good agreement with the experiments for the multilayer systems Nb/Cu and V/Ag, with various layer thicknesses.

DOI: 10.1103/PhysRevB.64.224526

PACS number(s): 74.50.+r, 74.76.-w

### I. INTRODUCTION

In trying to describe the experimental data for different kinds of multilayers, such as Nb/Cu or V/Ag, Koperdraad calculated upper critical magnetic fields versus temperature, using Takahashi-Tachiki theory for infinite multilayers.<sup>1</sup> He used as fitting parameters the bulk critical temperature of the S layer,  $T_c^S$ ; the ratio between the densities of states of the two materials,  $N_S/N_N$ ; and the two corresponding diffusion constants  $D_S$  and  $D_N$ .

In calculating the magnetic field anisotropy, which is the ratio between the parallel and perpendicular upper critical magnetic fields  $H_{c2,\parallel}/H_{c2,\perp}$ , two choices were possible for the diffusion constants, which led to two solutions, called the first and second solutions.<sup>2-7</sup> For the first solution, the fitted parameters are close to what one knows from the measurements. However, the dimensional crossover, typical for S/N multilayers, appeared to lie at a much higher temperature than the measured one. In the second solution the upper parallel critical magnetic field exhibits a dimensional crossover at a lower temperature than the experimental one. A characteristic of this type of solution is that the superconductivity nucleation point for the parallel magnetic field shifts from the S layer at low temperatures to the N layer at higher temperatures, which seems unphysical for a S/N multilayer whose  $T_c^N=0$ . Another unphysical aspect is that the fitted critical temperature for the S layer is larger than the one known for the bulk (8.9 K). Moreover, instead of an expected concave two-dimensional (2D) aspect of the curve at lower temperatures, the calculations lead to a convex type of curve. In order to fit the experimentally observed dimensional crossover with the theoretical one, Koperdraad and co-workers introduced a scaling parameter  $\alpha$  for the magnetic coherence length. However, the physical interpretation for this free parameter remains an open question.

Looking for a physical factor which can replace the role of the unphysical scaling parameter in fitting the data, Aarts<sup>8</sup> suggested to consider finite samples rather than the infinite ones on which Koperdraad and co-workers did their calculations. In finite samples one has to face surface effects. Model calculations done on finite samples<sup>9</sup> show that the surface nucleation of the superconductivity is more pronounced for multilayers with thinner layers, but it almost disappears as

one increases the thickness of the layers. Since the fitting problem mentioned above showed up particularly for thick-layer systems, taking into account surface superconductivity does not bring any essential improvement to the already existing results.

In the present paper we consider the influence of a S/N interface resistivity, in order to get rid of the unphysical parameter  $\alpha$ . This is in line with experimental evidence that the interfaces of artificial multilayers for metals with a different crystal structure such as Nb/Cu are quite rough.<sup>10</sup> Indeed, we find that a finite boundary resistivity ( $R_B$ ) allows for a good fit with the experimental data.

The paper is organized as follows. In Sec. II we summarize the theory of Takahashi and Tachiki, and we introduce the boundary resistivity by adjusting the boundary conditions. We also illustrate the role of the boundary resistivity on the proximity effect. Section III is dedicated to the numerical results and conclusion.

### II. THEORY INCLUDING BOUNDARY RESISTIVITY

First we summarize the Takahashi-Tachiki theory for S/N multilayers. The theory starts from the Gor'kov equation<sup>11</sup> for the pair potential  $\Delta(\mathbf{r})$ , with a space-dependent coupling constant  $V(\mathbf{r})$ ,

$$\Delta(\mathbf{r}) = V(\mathbf{r})kT \sum_{\omega} \int d^3\mathbf{r}' Q_{\omega}(\mathbf{r}, \mathbf{r}') \Delta(\mathbf{r}'), \quad (1)$$

in which the summation runs over the Matsubara frequencies. By averaging over the impurity configurations and considering the dirty limit, it was shown that the integration kernel  $Q_{\omega}$  obeys a Green's-function-like equation

$$[2|\omega| + L(\nabla)]Q_{\omega}(\mathbf{r}, \mathbf{r}') = 2\pi N(\mathbf{r})\delta(\mathbf{r} - \mathbf{r}'), \quad (2)$$

where

$$L(\nabla) = -\hbar D(\mathbf{r}) \left( \nabla - \frac{2ie}{\hbar c} \mathbf{A}(\mathbf{r}) \right)^2. \quad (3)$$

This result appears to be equivalent to a different approach going back to Usadel.<sup>7,12</sup> The material parameters  $V(\mathbf{r})$ ,  $N(\mathbf{r})$ , and  $D(\mathbf{r})$  are the BCS coupling constant, the electronic density of states at the Fermi energy, and the diffusion

coefficient, respectively. In practice, they are treated as being constant in each single layer. At the interfaces de Gennes boundary conditions are imposed,<sup>13</sup> which require the continuity of  $F(\mathbf{r})/N(\mathbf{r})$  and  $D(\mathbf{r})[\nabla - (2ie/\hbar c)\mathbf{A}(\mathbf{r})]F(\mathbf{r})$ , where the pair amplitude  $F(\mathbf{r})$  is related to the gap function  $\Delta(\mathbf{r})$  through

$$\Delta(\mathbf{r}) = V(\mathbf{r})F(\mathbf{r}). \quad (4)$$

Takahashi and Tachiki provide a way of solving Eqs. (1) and (2) by developing the kernel  $Q_\omega(\mathbf{r}, \mathbf{r}')$  and the pair function  $F(\mathbf{r})$  in terms of a complete set of eigenfunctions of the differential operator  $L(\nabla)$ . These eigenfunctions are labeled by the parameter  $\lambda$ , and the eigenvalues are  $\epsilon_\lambda$ . They are a solution of the eigenvalue problem

$$L(\nabla)\Psi_\lambda = \epsilon_\lambda \Psi_\lambda, \quad (5)$$

subject to de Gennes boundary conditions. The requirement of the existence of a solution for Eq. (1) leads to the equation

$$\det \left| \delta_{\lambda\lambda'} - 2\pi kT \sum_\omega \frac{1}{2|\omega| + \epsilon_\lambda} V_{\lambda\lambda'} \right| = 0. \quad (6)$$

For finite multilayers in vacuum, the de Gennes boundary conditions ensure that there is no current flow through the interface between the multilayer and the vacuum. These boundary conditions read  $D(\mathbf{r})[\nabla - (2ie/\hbar c)\mathbf{A}(\mathbf{r})]_z F(\mathbf{r}) = 0$  for the pair amplitude, at the interface with the vacuum. As usual for these type of layered systems, the growth direction coincides with the  $z$  direction. When applied to the eigenfunctions  $\Psi_\lambda$ , they become  $\partial\Psi_\lambda(x, y, z)/\partial z = 0$ , where we made use of the gauge  $\mathbf{A}(\mathbf{r}) = (Hz, 0, 0)$  when the magnetic field is applied parallel to the layers and  $\mathbf{A}(\mathbf{r}) = (0, Hx, 0)$  for the perpendicular magnetic field. In the absence of a magnetic field, the solution of Eq. (6) giving the largest value for the critical temperature is the physical one. In the presence of a field, solving this equation allows us to derive the  $H_{c2}(T)$  curves. The temperature at which  $H_{c2} \rightarrow 0$  is  $T_c$ .

A further step in applying the theory of Takahashi and Tachiki is to consider the effect of the S/N interface resistivity. In our calculations, we make use of more general boundary conditions rather than the de Gennes ones. Such boundary conditions were investigated by Kupriyanov and Lukichev<sup>14</sup> and according to Golubov and Kupriyanov<sup>15</sup> and Khushainov<sup>16</sup> they can be written as

$$\begin{aligned} D(\mathbf{r}) \frac{\partial}{\partial z} F(\mathbf{r}) \Big|_{\mathbf{r}=\mathbf{r}^+} &= D(\mathbf{r}) \frac{\partial}{\partial z} F(\mathbf{r}) \Big|_{\mathbf{r}=\mathbf{r}^-} \\ &= \frac{1}{e^2 R_B} \left( \frac{F(\mathbf{r}^+)}{N(\mathbf{r}^+)} - \frac{F(\mathbf{r}^-)}{N(\mathbf{r}^-)} \right). \end{aligned} \quad (7)$$

The boundary resistivity  $R_B$  is a parameter which characterizes the barrier which electrons encounter at the interface. A source of this resistance comes from the mismatch of the Fermi (or electronic) levels, lattice structure, and lattice constant of the two composite metals. As a consequence,  $R_B$

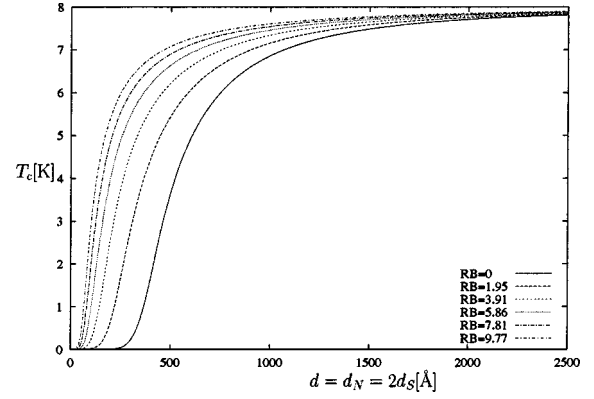


FIG. 1. The critical temperature  $T_c$  for an 11-layers Nb/Cu system, as a function of the layer thickness for different values of the boundary resistivity  $R_B$ , measured in  $\mu\Omega$  cm.

reduces the migration of the Cooper pairs from the S layer to the N layer, by that diminishing the proximity effect.

As we will illustrate in the following,  $R_B$  modifies the critical temperature  $T_c$  of the multilayer and the magnetic field anisotropy, defined as  $H_{c2,\parallel}/H_{c2,\perp}$ . By consequence, including  $R_B$  as a parameter, the two solutions used by Koperdraad and co-workers have to be reconsidered. It will turn out that in using the boundary resistivity as a free parameter, only one solution will be possible for the fitting, instead of two solutions. This solution fits the experimental data, without using any other free parameter, such as the scaling parameter  $\alpha$ .

Let us first consider the situation in which there is no magnetic field applied to the system. As mentioned already, a finite boundary resistivity reduces the proximity effect. This leads to a higher multilayer critical temperature than in the case of perfect transparency of the interfaces. As a consequence, the bulk critical temperature  $T_c^S$  used to fit the multilayer critical temperature will be smaller than the one used by Koperdraad and co-workers. This leads us in a good direction, since the previously used  $T_c^S$  was higher than the measured value.

As an illustration of the influence of  $R_B$  on the proximity effect, we calculate the dependence of the critical temperature of a multilayer on the thickness of the layers for different choices for the boundary resistivity. The results for an 11-layers Nb/Cu system are shown in Fig. 1. First, one notices that as the layer thickness decreases, the multilayer critical temperature converges smoothly towards 0, whereas in the thick layer limit, it converges to the bulk critical temperature  $T_c^S$ . Further, the curves show that below a certain thickness of the layers,  $d_{cr}$ , the superconductivity disappears. Moreover, this critical thickness  $d_{cr}$  decreases with the increasing of the boundary resistivity, illustrating the fact that due to  $R_B$ , the density of Cooper pairs is more localized in the S layers of the multilayer, so that the system becomes a better superconductor.

We consider now the presence of a magnetic field. When a magnetic field is applied to the system perpendicularly to the interfaces, due to the in-plane motion of the Cooper pairs, the influence of the boundary resistivity is weak. How-

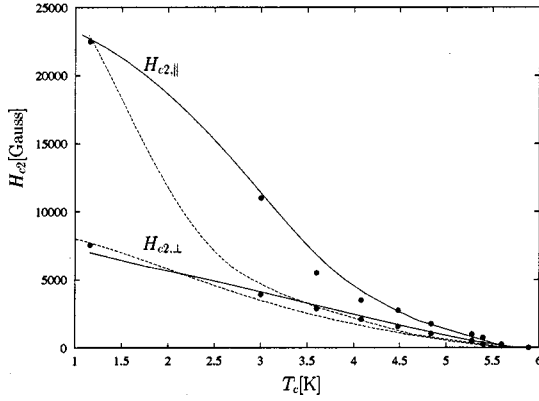


FIG. 2. The upper parallel and perpendicular magnetic fields for the multilayer Nb(171 Å)/Cu(376 Å). The dots denote the experimental points (Ref. 18).

ever, for the magnetic field parallel to the interfaces, the picture looks different. In this situation, the Cooper pairs move such that they cross the interface, which means that they experience the influence of the boundary resistivity much more strongly. In the presence of a boundary resistivity, the diffusion of the Cooper pairs from the S layers into the N layers is diminished. The proximity effect is weaker, leading to a higher critical temperature for the same magnitude of the magnetic field. Thus we can conclude that the boundary resistivity increases the anisotropy ratio  $H_{c2,||}/H_{c2,\perp}$ .

In addition it appears that the dimensional crossover temperature is shifted towards higher temperatures. This means that the first solution is not favorable, whereas the second solution has chances to be ameliorated.

In the following section we will take as a starting point the second solution and we will present the corrections which are performed in view of a fitting with the experimental data.

### III. RESULTS AND CONCLUSIONS

Considering the second solution, its inconveniences consist in the fact that at low temperature the  $H_{c2,||}(T_c)$  curve is convex, instead of the well-known concave square-root behavior for the 2D systems. Besides, at high temperatures the nucleation of the superconductivity lies in the N layer, which is unphysical for such S/N systems. Moreover, a too large ratio  $N_N D_N / N_S D_S$  is used in fitting, in order to obtain the corresponding anisotropy.

All these shortcomings are remedied by considering a finite boundary resistivity. In Fig. 2 we show results for a

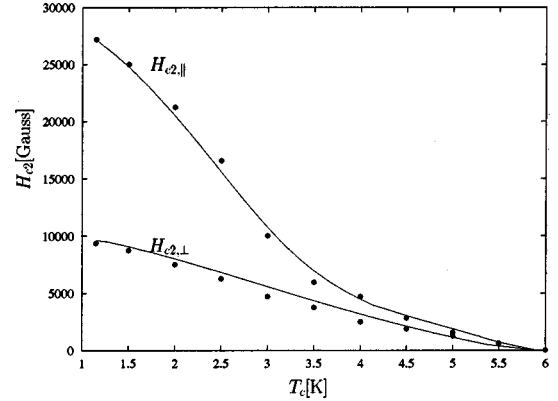


FIG. 3. The upper parallel and perpendicular magnetic fields experimental (Ref. 18) and theoretical curves for the multilayer Nb(172 Å)/Cu(333 Å).

Nb(171 Å)/Cu(376 Å) multilayer. The solid curves are obtained by accounting for a finite  $R_B$ . The dashed curves are the results of Koperdraad and co-workers, which could be improved by using a scaling parameter, still lacking a physical interpretation. The perpendicular field curves are not very sensitive to the change of the parameters. We fitted the points  $H_{c2}(T_{c2})=0$ ,  $H_{c2,||}(T^{DCO})$ , and  $H_{c2,\perp}(T^*)$  on the measured critical field curves, rather than the points  $H_{c2}(T_{c2})=0$ ,  $H_{c2,||}(T^*)$ , and  $H_{c2,\perp}(T^*)$ , used by Koperdraad and co-workers. Here  $T^{DCO}$  is the temperature where the dimensional crossover occurs on the parallel magnetic field curve, and  $T^*$  corresponds to the experimental point at the lowest temperature. In Table I, we show the data used in our fitting ( $T_c^S$ ,  $D_S$ ,  $D_N$ , and  $R_B$ ), compared to the data used by Koperdraad and co-workers ( $T_c^{S,K}$ ,  $D_S^K$ , and  $D_N^K$ ). For example, in fitting the Nb(171 Å)/Cu(376 Å) system, we used  $D_S = 2.4 \text{ cm}^2/\text{s}$ ,  $D_N = 78 \text{ cm}^2/\text{s}$ , and  $R_B = 3.17 \mu\Omega \text{ cm}$ , instead of  $D_S = 0.65 \text{ cm}^2/\text{s}$  and  $D_N = 138 \text{ cm}^2/\text{s}$ , used by Koperdraad and co-workers. The latter set is rather unrealistic, while the first set compares nicely with the diffusion constants used by Biagi *et al.*<sup>17</sup> The resistivity has the same order of magnitude as the resistivity of Nb at 77 K, which is  $\rho_{Nb} = 3 \mu\Omega \text{ cm}$ , and it is an order of magnitude larger than the Cu value of  $0.2 \mu\Omega \text{ cm}$ . Since the interface can be considered as a dirty mixture, the value of  $R_B$  looks reasonable. The use of a smaller and more realistic ratio  $N_N D_N / N_S D_S$  can be explained as follows. In the absence of a boundary resistivity,  $R_B = 0$ , the anisotropy at a certain temperature  $T^*$  is directly related to the ratio  $N_N D_N / N_S D_S$ . However, the anisotropy increases when one considers a finite  $R_B$ , so that a smaller ratio  $N_N D_N / N_S D_S$  is necessary to fit the anisotropy of the

TABLE I. Fitting data for the  $H_{c2}(T)$  curves, compared to the ones used by Koperdraad.

The system	$T_c$ [K]	$D_S$ [ $\text{cm}^2/\text{s}$ ]	$D_N$ [ $\text{cm}^2/\text{s}$ ]	$R_B$ [ $\mu\Omega \text{ cm}$ ]	$T_c^K$ [K]	$D_S^K$ [ $\text{cm}^2/\text{s}$ ]	$D_N^K$ [ $\text{cm}^2/\text{s}$ ]
Nb(171 Å) /Cu(376 Å)	9.20	2.4	78	3.17	9.89	0.65	138
Nb(172 Å)/Cu(333 Å)	9.20	1.23	69	2.07	9.88	0.64	180
Nb(168 Å)/Cu(147 Å)	9.50	1.45	73	2.38	9.61	0.58	231
V(240 Å)/Ag(480 Å)	5.47	1.1	54	3.52	5.70	0.67	73.4

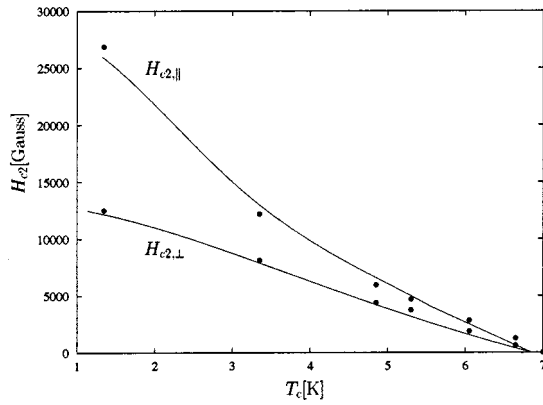


FIG. 4. The upper parallel and perpendicular magnetic fields experimental (Ref. 18) and theoretical curves for the multilayer Nb(168 Å)/Cu(147 Å).

upper critical fields. Besides, as one can notice in Fig. 2, this choice of the diffusion constants is such that the convex behavior of the  $H_{c2,||}(T)$  curve of Koperdraad and co-workers is turned into a concave one, characteristic for a 2D system. Furthermore, in our solution the nucleation of the superconductivity takes place in the S layer, as one expects for physical reasons. Clearly, good agreement between theory and measurements is obtained.

In the same way we fitted the data for two other Nb/Cu multilayers, as well as for a V/Ag system. The results are shown in Fig. 3 for Nb(172 Å)/Cu(333 Å), in Fig. 4 for Nb(168 Å)/Cu(147 Å), and in Fig. 5 for V(240 Å)/Ag(480 Å) multilayer. The experimental data are taken from

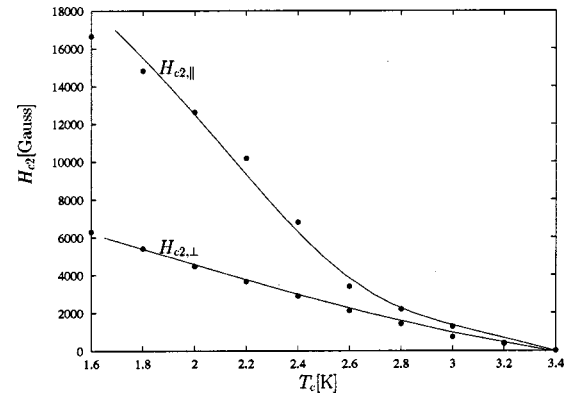


FIG. 5. The upper parallel and perpendicular magnetic fields experimental (Ref. 19) and theoretical curves for the multilayer V(240 Å)/Ag(480 Å).

the literature.<sup>18,19</sup>

In conclusion, by focusing on a fit at the dimensional crossover temperature and allowing for a finite boundary resistivity, the theory describes the experimental data nicely. By that the merit of the scaling parameter introduced by Koperdraad and co-workers is reduced considerably, the more so as up to now this parameter was not assigned any physical interpretation. A finite boundary resistivity, on the other hand, is in accordance with experimental evidence.<sup>10</sup>

#### ACKNOWLEDGMENTS

One of the authors (C.C.) would like to thank Dr. J. Aarts for useful discussions.

<sup>1</sup>S. Takahashi and M. Tachiki, Phys. Rev. B **33**, 4620 (1986); **34**, 3162 (1986).  
<sup>2</sup>A. Lodder and R.T.W. Koperdraad, Physica C **212**, 81 (1993).  
<sup>3</sup>R.T.W. Koperdraad and A. Lodder, Phys. Rev. B **51**, 9026 (1995).  
<sup>4</sup>R.T.W. Koperdraad, H.T. Wu, and A. Lodder, J. Phys.: Condens. Matter **8**, 8787 (1996).  
<sup>5</sup>R.T.W. Koperdraad and A. Lodder, Phys. Rev. B **54**, 515 (1996).  
<sup>6</sup>A. Lodder and R.T.W. Koperdraad, Physica C **212**, 81 (1993).  
<sup>7</sup>R.T.W. Koperdraad and A. Lodder, Physica C **268**, 216 (1996).  
<sup>8</sup>J. Aarts, Phys. Rev. B **56**, 8432 (1997).  
<sup>9</sup>C. Cihu and A. Lodder, cond-mat/0010445, Superlattices Microstruct. (to be published).  
<sup>10</sup>I.K. Schuller, Phys. Rev. Lett. **44**, 1597 (1980).

<sup>11</sup>L.P. Gor'kov, Sov. Phys. JETP **10**, 998 (1960).  
<sup>12</sup>K.D. Usadel, Phys. Rev. Lett. **25**, 507 (1970).  
<sup>13</sup>P.G. de Gennes, Rev. Mod. Phys. **36**, 225 (1964).  
<sup>14</sup>M.Y. Kupriyanov and V.F. Lukichev, Sov. Phys. JETP **67**, 1163 (1988).  
<sup>15</sup>A.A. Golubov and M.Y. Kupriyanov, Sov. Phys. JETP **69**, 805 (1989).  
<sup>16</sup>M.G. Khushainov, JETP Lett. **53**, 579 (1991).  
<sup>17</sup>K.R. Biagi, V.G. Kogan, and J.R. Clem, Phys. Rev. B **32**, 7165 (1985).  
<sup>18</sup>C.S.L. Chun, G-G. Zheng, J.L. Vincent, and I.K. Schuller, Phys. Rev. B **29**, 4915 (1984).  
<sup>19</sup>K. Kanoda, H. Mazaki, N. Hosoito, and T. Shinjo, Phys. Rev. B **35**, 6736 (1987).